

# Ultrastrong Poly(2-Oxazoline)/Poly(Acrylic Acid) Double-Network Hydrogels with Cartilage-Like Mechanical Properties

Paola A. Benitez-Duif, Marina Breisch, Daniel Kurka, Karlina Edel, Semra Gökçay, Dominic Stangier, Wolfgang Tillmann, Montasser Hijazi, and Jörg C. Tiller\*

The exceptional stiffness and toughness of double-network hydrogels (DNHs) offer the possibility to mimic even complex biomaterials, such as cartilage. The latter has a limited regenerative capacity and thus needs to be substituted with an artificial material. DNHs composed of cross-linked poly(2-oxazoline)s (POx) and poly(acrylic acid) (PAA) are synthesized by free radical polymerization in a two-step process. The resulting DNHs are stabilized by hydrogen bridges even at pH 7.4 (physiological PBS buffer) due to the  $pK_a$ -shifting effect of POx on PAA. DNHs based on poly(2-methyl-2-oxazoline), which have a water content (WC) of around 66 wt% and are not cytotoxic, show biomechanical properties that match those of cartilage in terms of WC, stiffness, toughness, coefficient of friction, compression in body relevant stress conditions and viscoelastic behavior. This material also has high strength in PBS pH 7.4 and in egg white as synovial liquid substitute. In particular, a compression strength of up to 60 MPa makes this material superior.

cause of disability for 500 million people worldwide, around 7% of the global population, and it is expected that the number of people affected by this condition will considerably increase in the coming years.<sup>[1,2]</sup>

Currently, there are several treatment strategies to mitigate the effects of cartilage damage, such as non-pharmacological methods (i.e., weight loss), pharmacological methods (e.g., Non-Steroidal Anti-Inflammatory Drugs)<sup>[1]</sup> and surgery interventions such as macrofracturing and Autologous Chondrocyte Implantation.<sup>[3,4]</sup> However, most of the treatment strategies mentioned above are still not a long-term solution to this condition. Due to the articular cartilage's complex structure the implementation of a suitable medical treatment remains a challenge. On one

hand, the articular cartilage structure is highly compacted and has no vascularity. This makes delivery of drug molecules to the tissue unfeasible. On the other hand, the cartilage lacks a fully self-healing capability and is a non-neural tissue, which means that symptoms appear when the cartilage damage is already severe.<sup>[5]</sup> In some cases, the only treatment left is a hip or a knee joint replacement upon detection. Nevertheless, approximately 90 to 95% of all joint replacements have an endurance time limited to 10 years.<sup>[4]</sup> Typically, mechanical failure of the implant material is the main reason for a new surgical intervention, which increases not only the burden of disease, but also the cost of treatment. Complications related to implant failure could still be prevented through the implementation of materials with long-term stable mechanical properties that could increase the functionality and the period of use.

The development of materials with cartilage-like features has steadily gained significance in the recent years. Since articular cartilage has a load bearing function with compressive strength values from 14 MPa up to 59 MPa,<sup>[6,7]</sup> an equilibrium water content (EWC) between 60 and 85 wt%,<sup>[4,5,8]</sup> as well as a very low Coefficient of Friction (COF) (0.001–0.5)<sup>[9]</sup>; developing of materials that mimic these biological features is highly challenging. Novel hydrogels systems,<sup>[10]</sup> such as double-network (DN) hydrogels,<sup>[4,11–14]</sup> fiber-reinforced DNs,<sup>[6]</sup> nanocomposite hydrogels,<sup>[15–17]</sup> and Extracellular Matrix (ECM)-based materials<sup>[18]</sup> have been developed in the recent years in order to obtain materials with highly tough mechanical properties

## 1. Introduction

Osteoarthritis (OA) is one of the most prevalent diseases affecting, inter alia, the articular cartilage (AC) in load bearing joints like hip, shoulder and knee. OA is currently a leading

P. A. Benitez-Duif, D. Kurka, K. Edel, S. Gökçay, M. Hijazi, J. C. Tiller  
Biomaterials and Polymer Science  
Department of Bio- and Chemical Engineering  
TU Dortmund University  
Emil-Figge-Str. 66, 44227 Dortmund, Germany  
E-mail: joerg.tiller@tu-dortmund.de

M. Breisch  
BG University Hospital Bergmannsheil Bochum  
Surgical Research  
Ruhr University Bochum  
Buerkle de la Camp Platz-1, 44789 Bochum, Germany

D. Stangier, W. Tillmann  
Institute of Materials Engineering  
TU Dortmund University  
Leonhard-Euler-Straße 2, 44227 Dortmund, Germany

 The ORCID identification number(s) for the author(s) of this article can be found under <https://doi.org/10.1002/adfm.202204837>.

© 2022 The Authors. Advanced Functional Materials published by Wiley-VCH GmbH. This is an open access article under the terms of the Creative Commons Attribution License, which permits use, distribution and reproduction in any medium, provided the original work is properly cited.

DOI: 10.1002/adfm.202204837

and tissue-like water content (WC).<sup>[10,19]</sup> Among all these materials, double-network hydrogels (DNHs) with at least one polyelectrolyte component such as salts of poly(2-acrylamido-2-methylpropanesulfonic acid)(PAMPS)<sup>[6,12,20–23]</sup> and poly(acrylic acid) (PAA)<sup>[24–28]</sup> have been particularly highlighted as potential cartilage-like materials. Thus, the incorporation of ionic components into the network leads not only to a better hydration of the hydrogel, but also to the improvement of the mechanical properties by hydrogen bonding and/or ionic interactions between the polymers involved.<sup>[10,13,19,29,30]</sup> Several double networks systems as promising artificial cartilage has been reported, many of them have been based on the work done by Gong,<sup>[31]</sup> in which PAMPS/PAAm DN gels with a WC of 90 wt% could bear up to 17 MPa of compressive stress. Means et al.<sup>[12]</sup> showed a DN hydrogel based on PAMPS/(PNIPAAm-co-AAm) with cartilage-like performance, with compressive strength of 25 MPa and WC values between 80–85 wt%. Ding et al.<sup>[24]</sup> reported a hydrogel composite of P(AA<sub>0.35</sub>-co-AM<sub>2.0</sub>)/XG<sub>1.0</sub>-GG<sub>1.0</sub>/Fe<sup>3+</sup>/B, which exhibited a compression strength above 15.3 MPa and a water uptake up to 72 wt%. The mechanical behavior of both mentioned systems were determined in distilled water; however, only the group of Wiley<sup>[6]</sup> has recently presented a system based on bacterial cellulose, PVA, and PAMPS, which has cartilage-like performance in the more physiologically relevant medium 0.15 M PBS buffer. This material takes up around 55 wt% of water and shows a compression strength of 173 MPa similar to the natural idol and an exceptional wear resistance.

Although these materials are very promising, the water uptake and therefore the mechanical properties of polymer networks with ionic components strongly vary with environmental conditions, such as pH and ion/salt concentration.<sup>[28,32,33]</sup> Thus, environmental changes during the in vivo implementation could cause problems, because the ionic network materials can change their dimensions and mechanical behavior in presence of fluids such as blood.

We presume that the most suitable material for cartilage replacement would be one that does not undergo great variation in either water-uptake or mechanical performance upon environmental changes. Such material would be more easily handled and would not substantially change dimensions or functionality upon implementation. In this work, we report on novel DNHs based on poly(2-oxazoline)s (POx) and non-ionized PAA with excellent mechanical cartilage-like behavior as potential new materials for artificial cartilage in varying physiologically relevant media.

## 2. Results and Discussion

Goal of this work was to create a DN hydrogel with cartilage-like mechanical properties in physiological environments, which are not strongly affected by the concentration of salts and other compounds. Thus, the double network should facilitate strong reversible bonds, such as hydrogen bridges, but no ionic functions. A strong hydrogen bond former is PAA, which has already been used as component to create stiff and strong physically cross-linked DN hydrogels with potential biomedical applications.<sup>[32,34–36]</sup> However, PAA based networks tend to

lose their excellent mechanical behavior in non-acidic environments, because the carboxylic acid groups of PAA are mostly deprotonated in aqueous medium with a pH-value above pK<sub>a</sub> 4.7. In consequence, the formation of H-bonds between the networks involved are impaired. For example, previously reported DNHs based on PAA and PEG showed excellent mechanical strength at pH values up to pH 4, but above this a dramatic reduction of the strength was observed.<sup>[28,37]</sup> Interestingly, it has been reported that the pK<sub>a</sub> value of PAA can be shifted to higher values in the presence of polymer networks with hydrophobic components, or a high degree of hydrogen bonding between the networks.<sup>[38,39]</sup> Several studies have emphasized the capability of POx to form stable hydrogen bonds with PAA or tannic acid (TA), particularly in layer-by-layer (LbL) systems.<sup>[38,40–42]</sup> Thus, these systems are more stable at higher pH values.

We have explored, if this is valid for DN hydrogels based on these two polymers (see **Figure 1**). To this end, telechelic poly(2-methyl-2-oxazoline) (PMOx) and poly(2-ethyl-2-oxazoline) (PEtOx) with acrylate end groups and different degree of polymerizations (25, 50, 100) were prepared by cationic ring-opening polymerization followed by end-group modification with *N*-[3-(Dimethylamino)propyl]methacrylamide (DMAP-MAA). Such end group functionalized POx have already been successfully used to form POx based homo-networks or amphiphilic conetworks.<sup>[43–46]</sup> All polymers could be obtained with narrow molecular weight distributions and nearly complete end group functionalization (see Table S1, Supporting Information).

The telechelic POx were cross-linked as films from their aqueous solutions via photo-polymerization. These primary networks were thoroughly rinsed in water for around 24 h, which is important to obtain a homogenous material in the end. Then, the single POx networks were soaked with acrylic acid containing photoinitiator and crosslinking agent (tetraethylene glycol dimethacrylate, TEGDMA) and these swollen hydrogels were again subjected to photopolymerization. The final DNHs were washed with water for at least 48 h and then given to a high access of the aqueous test medium and conditioned for at least another 48 h. The obtained DN hydrogels are transparent, bendable materials (see **Figure 1**).

The WC of articular cartilage is estimated to be 60 to 85 wt%. Water enables the exchange of nutrients, salts and, other metabolites through the cartilage matrix<sup>[47]</sup> and its content is used as indicator for cartilage damage.<sup>[48]</sup> It was observed that the water uptake of the POx/PAA hydrogels is mainly controlled by the degree of polymerisation of the macromonomer, that is, by theoretical mesh size of the primary POx-single network. DNHs based on POx macromonomers with a degree of polymerisation of 25 exhibited WCs with values of 48 ± 4 wt% for PMOx<sub>25</sub> and 50 ± 2 wt% for PEtOx<sub>25</sub> in PBS (pH 7.4) solution, which are too low and consequently not suitable to be used as cartilage replacement. DNHs based on PMOx with 50 and 100 repeat units showed WC values between 66 ± 3 and 88 ± 1 wt% in PBS, which corresponds to the WC-range of articular cartilage. The respective PBS-swollen PEtOx<sub>50</sub>/PAA DNH contains 59 ± 6 wt% of water and 74 ± 1 wt% for PEtOx<sub>100</sub>/PAA, which is most likely due to the less hydrophilic character of PEtOx. All highly PBS swellable DNHs were subjected to mechanical testing (see **Figure 2**).

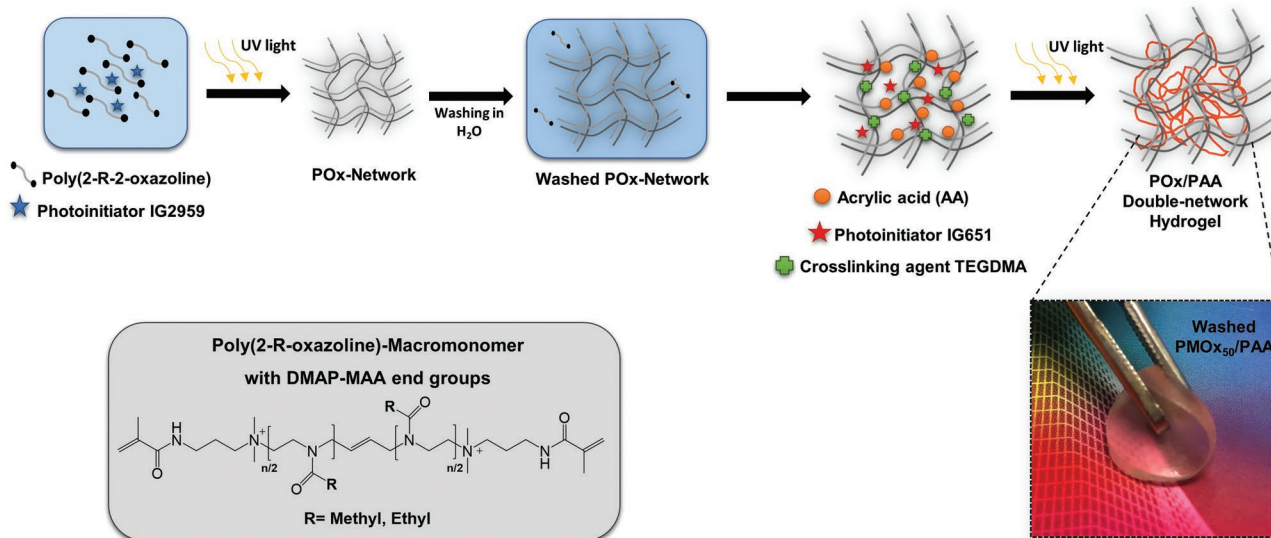


**Figure 1.** Steps of the synthesis of POx/PAA double-networks hydrogels.

As seen in Figure 2, only DNHs composed of POx with a degree of polymerization of 50 show a stiffness in PBS of around 3 MPa, which might be suitable for artificial cartilage, while the DNHs based on the respective polymers with 100 repeating units are not stiff enough for this purpose. Interestingly, the significantly less swollen PEtOx<sub>50</sub>-based DNH

does not exhibit a higher stiffness compared to the respective PMOX<sub>50</sub>-based system. This might be due to the less strong hydrogen bridges formed between PAA and PEtOx. A different scenario is found, when determining the tensile fracture energy. This experiment includes the propagation of a crack in the stress-strain experiment. As seen in Figure 2D, the tensile

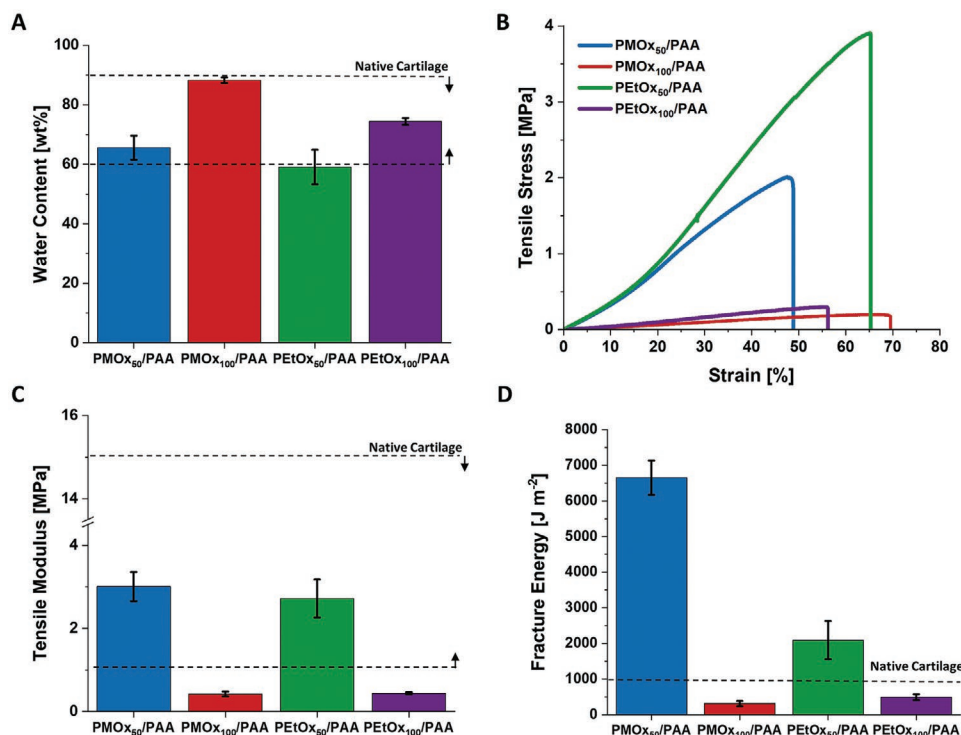


**Figure 2.** A) WC, B) initial tensile stress–strain curve, C) tensile modulus, D) fracture energy of DNHs PMOX<sub>50</sub>/PAA, PMOX<sub>100</sub>/PAA, PEtOX<sub>50</sub>/PAA, and PEtOX<sub>100</sub>/PAA in PBS (pH 7.4) media. The corresponding literature values for WC,<sup>[4,5,8]</sup> initial tensile modulus,<sup>[49,50]</sup> and fracture energy<sup>[15]</sup> of native articular cartilage are indicated by black lines. Values in (A,C,D) are expressed as mean ± SD (*n* = 4–5). The tensile stress–strain curves are recorded with a strain rate of ≈0.001 s<sup>-1</sup>. The reference values for cartilage from the literature are recorded at similar strain rates.

fracture energy of the PMOx<sub>50</sub> system is with  $6.9 \pm 0.7 \text{ kJ m}^{-2}$  exceptionally high. In contrast, the PEtOx<sub>50</sub>/PAA DNH exhibits a tensile fracture energy of  $2.1 \pm 0.5 \text{ kJ m}^{-2}$ , which is much lower than that of the PMOx<sub>50</sub> system, but still higher than that of natural cartilage ( $1 \text{ kJ m}^{-2}$ ).<sup>[15]</sup> This might be explainable by the fact that the PEtOx system is not as homogeneous as the respective PMOx-based DNH. This can cause an easier crack propagation. In comparison, DNH PMOx<sub>100</sub>/PAA and PEtOx<sub>100</sub>/PAA showed a poor mechanical behavior when stretched.

Based on these results, it can be assumed that the interactions by hydrogen bonds between the segments of PAA and PMOx inside the network serve as sacrificial bonds in order to dissipate the mechanical stress effectively, leading to DNHs with remarkable toughness. The cross-linking density of the primary POx network can control the mechanical properties and water-uptake of the DNH. Particularly, the PMOx<sub>50</sub>/PAA DNH shows a WC, stiffness and fracture energy in physiological PBS that makes it a promising candidate for artificial cartilage. Only this material was subjected to further experiments.

Cartilage is a load-bearing tissue with compressive strength values between 15 and 57 MPa.<sup>[6]</sup> Mimicking of close to real physiological conditions is often performed in PBS buffer at pH 7.4, because it has the salt concentration and the pH of blood. However, the cartilage is surrounded by synovial fluid, which not only transports nutrients inside of the cartilage, but also supports the lubricity and has a cushioning-effect.<sup>[51]</sup> It is well known that egg white has similarities to the synovial fluid regarding consistence<sup>[52]</sup> and also containing glycosaminoglycans (GAGs), such as chondroitin sulfate, hyaluronic acid and keratan sulfate, which are also part of the cartilage structure/composition and play a fundamental role in the mechanical behavior of cartilage.<sup>[4,5,53]</sup> Many studies have shown interest on hen egg white as source of exogenous GAGs such as keratin sulfate, in order to suppress the cartilage damage.<sup>[54–56]</sup> Thus, we performed the compressive test not only in PBS, but also in egg white, in order to observe the effect of GAGs in the mechanical behavior of the DNHs.

As seen in Figure 3A, PMOx<sub>50</sub>/PAA in both media—PBS and egg white—exhibits a compression profile similar to articular

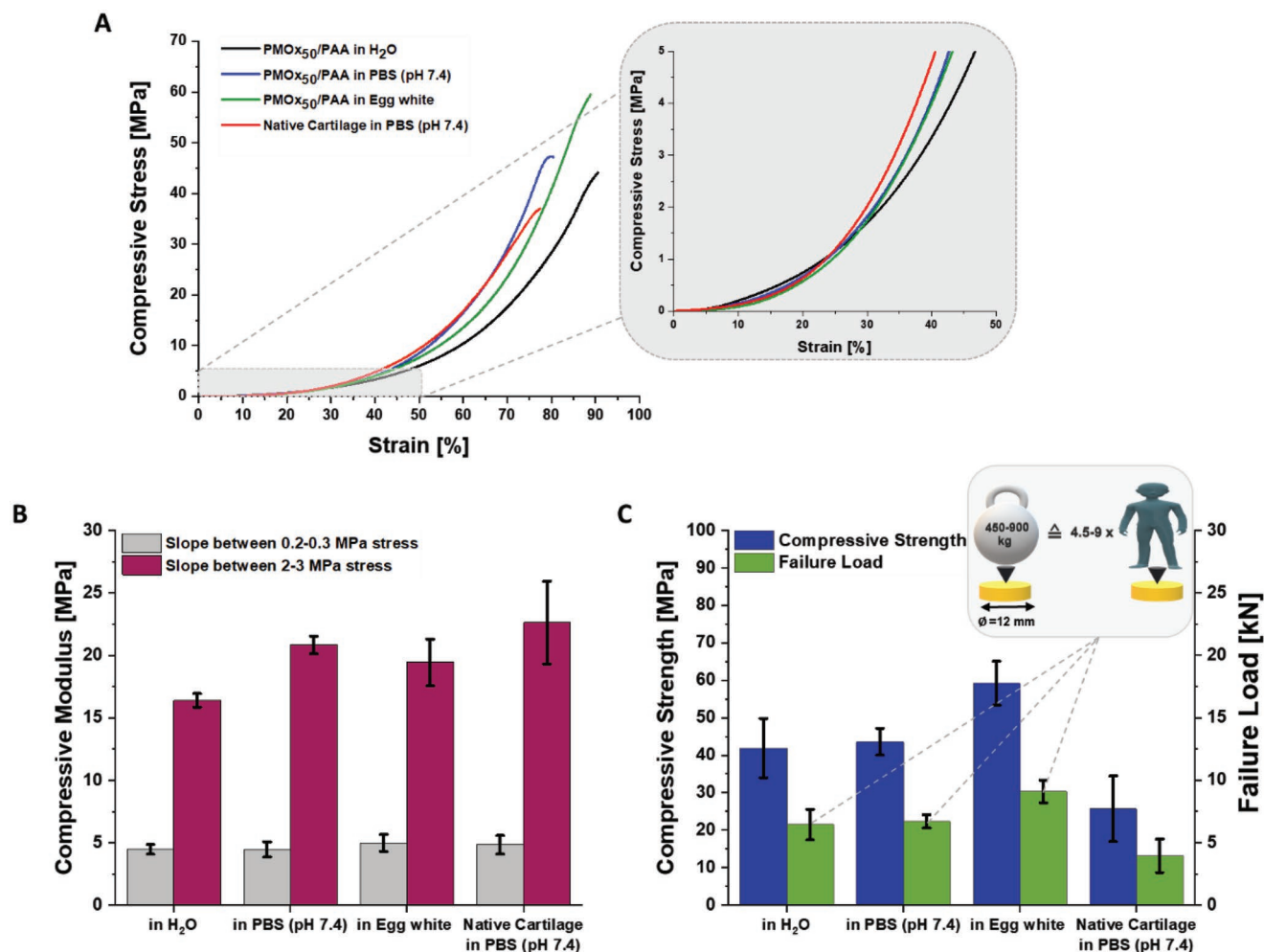


**Figure 3.** A) Compressive stress–strain curve, B) compressive strength and compressive modulus, C) failure load of native cartilage in PBS (pH 7.4) and PMOx<sub>50</sub>/PAA in PBS (pH 7.4), and egg white media. The samples have a diameter of 12 mm and an average thickness of  $2 \pm 0.2 \text{ mm}$ . The compressive stress–strain curves are recorded with a strain rate of  $0.0043 \text{ s}^{-1}$ . Values in (B,C) are expressed as mean  $\pm$  SD ( $n = 5$ ).

cartilage. The compression moduli were determined from the slopes of the compression profiles in two different stress ranges 0.2–0.3 MPa and 2–3 MPa. Both ranges are relevant; thus, it has been documented, that the contact stress of articular cartilage can reach values between 0.02–5 MPa.<sup>[8,12,57]</sup> As seen in Figure 3B, the compression moduli at a stress of 2–3 MPa of PMOx<sub>50</sub>/PAA are 20.8 ± 0.7 MPa in PBS and 19.4 ± 1.8 MPa in egg white, which are both not significantly lower than that of articular cartilage with 22.6 ± 3.3 MPa. Noticeably, the GAGs in egg white do not influence the compression modulus of the material compared to those in PBS. The DNH also shows a similar compression modulus in water. The compression modulus values of both materials also do not exhibit significant differences at lower stress ranges. The same effect was observed after the treatment of the DNH with the hydrolase-enzyme Lipase, which can be found in human blood (for details see supporting information). Thus, this ubiquitous hydrolase cannot easily degrade the hydrogel.

The compressive strength values of PMOx<sub>50</sub>/PAA are 45 MPa in PBS and 60 MPa in egg white and thus both exceed that of the measured native articular cartilage in PBS (29.6 ± 8.7 MPa). Considering, that the DNH has a WC of 67 wt% in egg white, its compression strength in egg white is remarkably high. We thus assume that the GAGs in egg white have not only a shock absorber functionality, but also play a role as a third network, which protects the hydrogel from the compressive stress. Cartilage is known to have the capability to resist loads of several times the body weight.<sup>[58]</sup> The PMOx<sub>50</sub>/PAA DNH can bear even higher loads between 450 and 900 kg, which implies the withstanding of 4.5 up to 9 times of a body weight of 100 kg in a surface area of 113 mm<sup>2</sup> (see Figure 3C), which makes this DNH a promising material with an extraordinary compressive mechanical performance.

Cartilage is a material that needs to withstand always varying mechanical stress. Therefore, the mechanical properties of PMOx<sub>50</sub>/PAA hydrogels were further explored by applying a sequential dynamic movement profile. The parameter of interest in such an experiment is to determine if the material shows plastic deformation (creep) and how fast it recovers to its original state. Moreover, the mechanical properties of the material after the dynamic stress experiment are of interest. The experiment was started with a creep test applying a total constant force of 8.7 N (≈0.3 MPa, typical load of the human knee) to simulate the standing position for 30 min. In order to simulate the gait movement, a static force of 8.7 N and a dynamic force of 8.5 N (total stress ≈0.6 MPa) with a frequency of 1 Hz was applied for another 30 min. A frequency of 1 Hz has been reported as characteristic gait frequency.<sup>[59]</sup> Afterwards, the material was kept at 0.3 MPa for 3 min (standing) and then the load was removed (see Figure 4A). The thickness or rather the strain of the material was measured after 1 s unloading and again after 1800 s of recovery (Figure 4B,C).

As seen in Figure 4C the DNH exhibits in both media – PBS and egg white – a higher instantaneous recovery of its initial thickness than native cartilage. However, after 30 min both materials showed a no significant difference of their thickness recovery with values of 53 ± 11%, 59 ± 9% and 61 ± 9% for the native cartilage, DNH in egg white and in PBS, respectively. One reason for the faster recovery of the PMOx<sub>50</sub>/PAA

hydrogels could be linked to the differences of the compressive modulus before and after the load exposure (see Figure 4D). The PMOx<sub>50</sub>/PAA exhibited a slight increase of their compressive modulus compared to cartilage. Thus, the DNH in the different media was not as strongly deformed by the load as cartilage, and so can recover more quickly. The slow deformation recovery of cartilage compared to DNHs has been also observed in a work of Grunlan et. al,<sup>[12]</sup> in which PAMPS/P(NIPAAm-co-AAm) DNHs and cartilage were subject to a creep test with a compressive stress of 0.35 MPa for 1 h. While the DNH showed recovery strains above 70% immediately after removal of the load, a recovery strain of 6–8% was observed for cartilage. After 30 min of recovery, cartilage and the PAMPS/P(NIPAAm-co-AAm) exhibited recovered strain values between 80–90%.

Having established that the PMOx<sub>50</sub>/PAA shows mechanical properties similar to native cartilage, it was now investigated, whether the material also possesses a low COF, which is a crucial characteristic of the natural biomaterial. To this end, the DN hydrogels were swollen in PBS (pH 7.4) and egg white, respectively, and subjected to a tribological test applying a load of 5 N (maximum Hertzian contact stress 1.2 MPa) with a sliding velocity of 5 mm s<sup>-1</sup> at room temperature for 1 h (375 laps with a stroke length of 8 mm).

As seen in Figure 5A the DNH has a COF in PBS of 0.11 and in egg white of 0.07. Both values are well in the range of COFs given for natural cartilage in the literature. The kinetics of the friction experiment shown in Figure 5B indicates that the COF quickly drops at the beginning in both media. In the case of PBS (pH 7.4) as medium, the friction coefficient slightly increases with time, while the COF in egg white remains constant after the initial drop. The lower friction of the DN hydrogels in egg white confirms the suitability of the latter as synovial fluid substitute, which is responsible for the low friction of cartilage in the body. The tribological test also confirms the remarkable mechanical performance of the PMOx<sub>50</sub>/PAA DNHs in relevant physiological media.

As already mentioned a particularity of networks with poly-electrolyte components is the response of the swelling and mechanical behavior to changes in the salt content and in the pH value of the swelling media. In order to avoid this, we choose the system POx and PAA, because the strong hydrogen bonds between those two would increase the pK<sub>a</sub> value of PAA. Thus, the DNH might not be deprotonated even in physiological environments and would thus retain its excellent mechanical properties. In order to confirm this and to explore the limitations of the material, the PMOx<sub>50</sub>/PAA hydrogels were conditioned in media with varying the pH value of PBS solution for one week and the degree of swelling and the compressive strength was determined (see Figure 6).

As seen in Figure 6, the water uptake of the DNH in water, PBS (pH 7.4), and egg white, respectively, is nearly identical in a range of 61–67 wt%. The compressive strength is similar in water and PBS, clearly showing that salt concentration and a pH of up to 7.4 do not affect the material. Increasing the pH value in PBS to 7.6 results in increased water uptake of 70 wt% and a drop in strength to almost half (24.4 MPa) the value at pH 7.4. Further increasing the pH to 8.0 and 8.5 results in an increased water uptake and a somewhat less dramatic drop in strength. In order to find, what causes the pH-induced changes

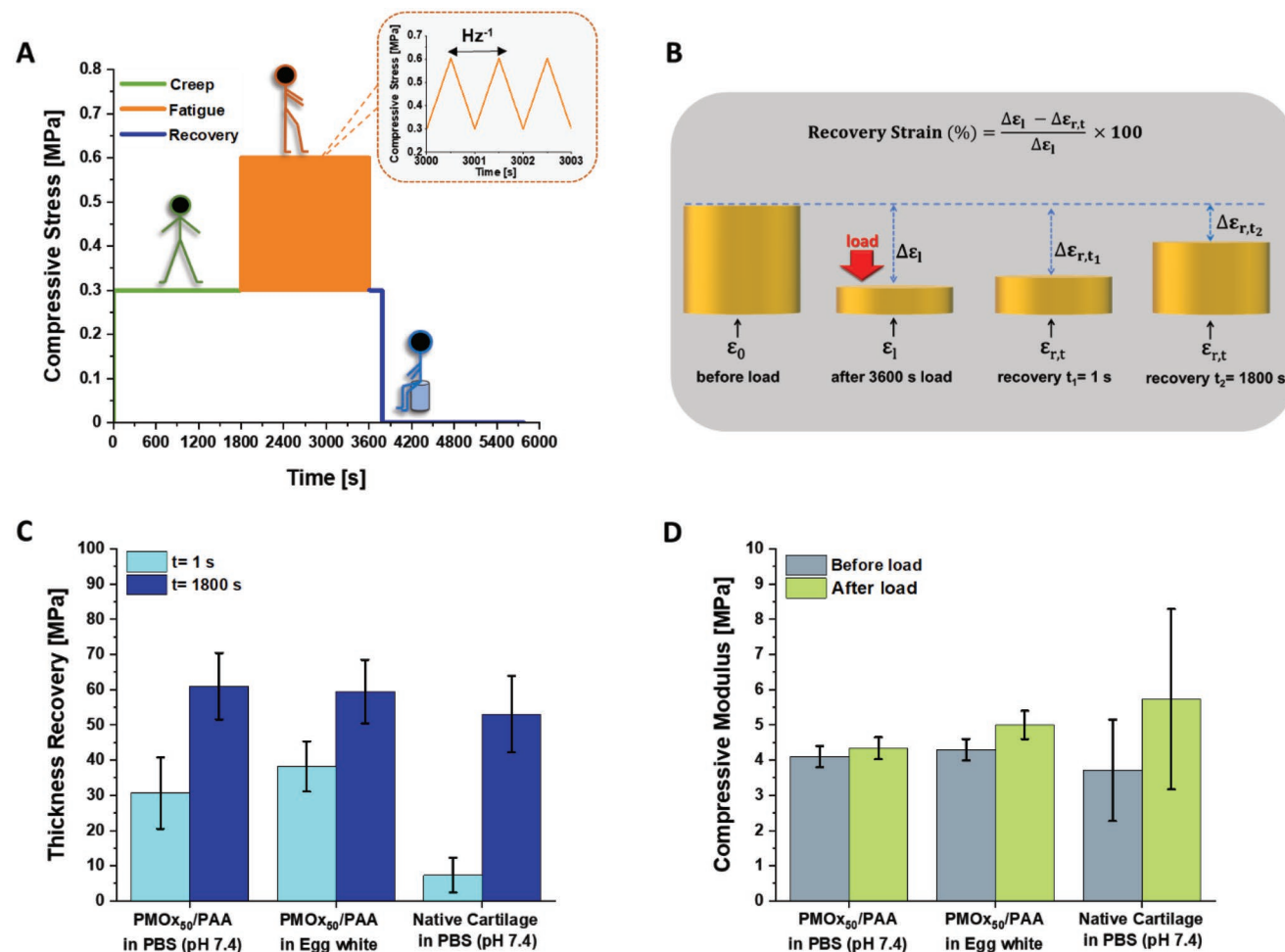


**Figure 4.** A) Viscoelasticity test (creep, fatigue, and recovery), B) illustrated determination of the recovery strain, C) recovery strain and D) compressive modulus of native cartilage in PBS (pH 7.4) and PMOx<sub>50</sub>/PAA in PBS (pH 7.4) and egg white media. The samples have a diameter of 6 mm and an average thickness of  $1.8 \pm 0.2$  mm. Values in (C,D) are expressed as mean value  $\pm$  SD ( $n = 5$ ).

in swelling and strength, FTIR spectra of PMOx<sub>50</sub>/PAA in media with different pH values were recorded (see Figure 7).

As seen in the top of Figure 7, the FTIR spectrum of a PAA single network exhibits the characteristic peak of the stretching

vibration of the C = O function of the protonated carboxylic acid at  $1697 \text{ cm}^{-1}$ . When treating this PAA network with PBS buffer, pH 7.4 overnight, the FTIR spectrum of the dried material is significantly changed as seen by the appearance of two new

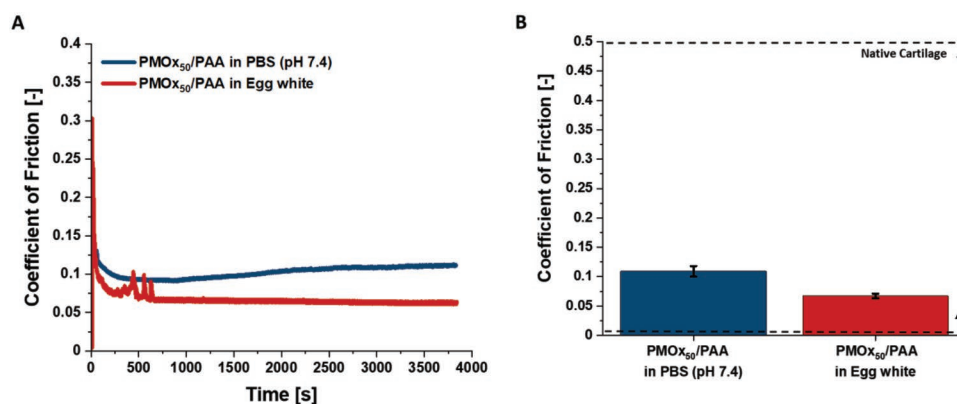


**Figure 5.** A) COF versus time and B) COF of PMOx<sub>50</sub>/PAA in PBS (pH 7.4) and egg white as swelling media and lubricant. The black lines indicate the corresponding native articular cartilage values.<sup>[9]</sup> Values in (B) are expressed as mean value  $\pm$  SD ( $n = 4$ ).

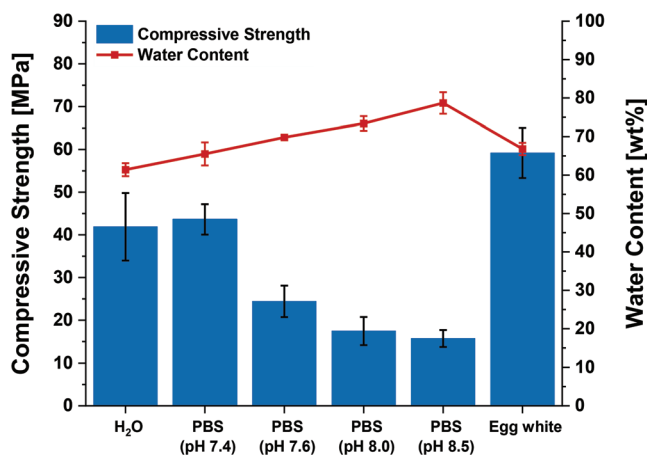


**Figure 6.** Effect of the pH-value on the mechanical performance of PMOx<sub>50</sub>/PAA. All materials are swollen in a high excess of the respective medium at room temperature for at least 48 h before determining the mechanical performance in the corresponding medium. The samples have a diameter of 12 mm and an average thickness of  $2 \pm 0.2$  mm. Values are expressed as mean value  $\pm$  SD ( $n = 5$ ).

peaks at 1640 and 1539  $\text{cm}^{-1}$ , which are typical for the deformation vibrations of C-OH and the symmetrical stretching of  $\text{COO}^-$  of the salt form of PAA.<sup>[60,61]</sup> The still existing peak at 1701  $\text{cm}^{-1}$  of the protonated carboxylic group indicates that the deprotonation of PAA is not complete in PBS, pH 7.4. The third spectrum from the top of Figure 7 is of the PMOx single network with the typical C = O stretching vibration at 1607  $\text{cm}^{-1}$ . The FTIR spectrum of the PMOx<sub>50</sub>/PAA washed with water is characterized by two dominant peaks at 1705 and 1589  $\text{cm}^{-1}$ . The first signal can be attributed to the carboxylic acid function of PAA, while the second peak is the red-shifted peak of the

C = O stretching vibration of PMOx. This red shift is a strong indicator of the formation of hydrogen bridges between PMOx and PAA including all C = O functions of the first. This DNH was soaked in PBS, pH 7.4, overnight and dried. The FTIR spectrum of this network looks exactly the same as that of the DNH just treated with water, indicating that no deprotonation of the acid functions occurs in contrast to the free PAA network. Next, the DNH was soaked in PBS, pH 7.6, overnight and dried. The FTIR spectrum of this material shows a new signal at 1540  $\text{cm}^{-1}$ , which is attributed to the salt form of PAA and an almost complete disappearance of the signal at 1590  $\text{cm}^{-1}$ , which is the marker for the hydrogen bonds. These results show that the combination of PAA and PMOx in a DNH results in a dramatic apparent increase in the  $\text{pK}_a$  value of PAA due to strong hydrogen bond formation. The DNH does not deprotonate in PBS pH 7.4 and thus retains its excellent mechanical strength in this environment. However, increasing the pH to only 7.6 leads to strong deprotonation and a drastic drop in strength due to the destruction of the hydrogen bonds.

## 2.1. Cytocompatibility

In addition to the mechanical behavior, another important aspect of the implementation of an artificial material is its cytocompatibility. PAA is a well-known biocompatible material. POx is also discussed to be biocompatible. However, there are studies that show that POx with certain end groups can be enzyme inhibitors.<sup>[62,63]</sup> On the other hand, modification of proteins with POx does not deactivate the enzymes.<sup>[64,65]</sup> Therefore, it is necessary to explore the cytotoxicity of the POx-based material. To this end, the PMOx<sub>50</sub>/PAA samples were placed in a Petri dish only covering a part of the bottom. Then human mesenchymal stem cells (hMSC) were placed on top and incubated

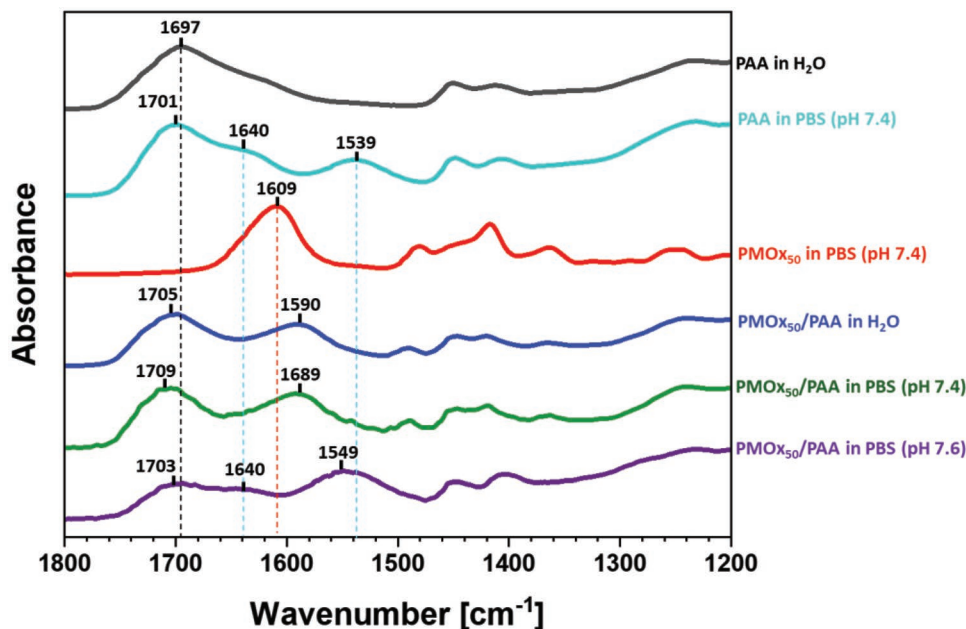


**Figure 7.** FTIR-spectra of the single networks, PAA and PMOx<sub>50</sub>, and PMOx<sub>50</sub>/PAA DNHs in H<sub>2</sub>O and in PBS at pH-values between 7.4 and 8.5.

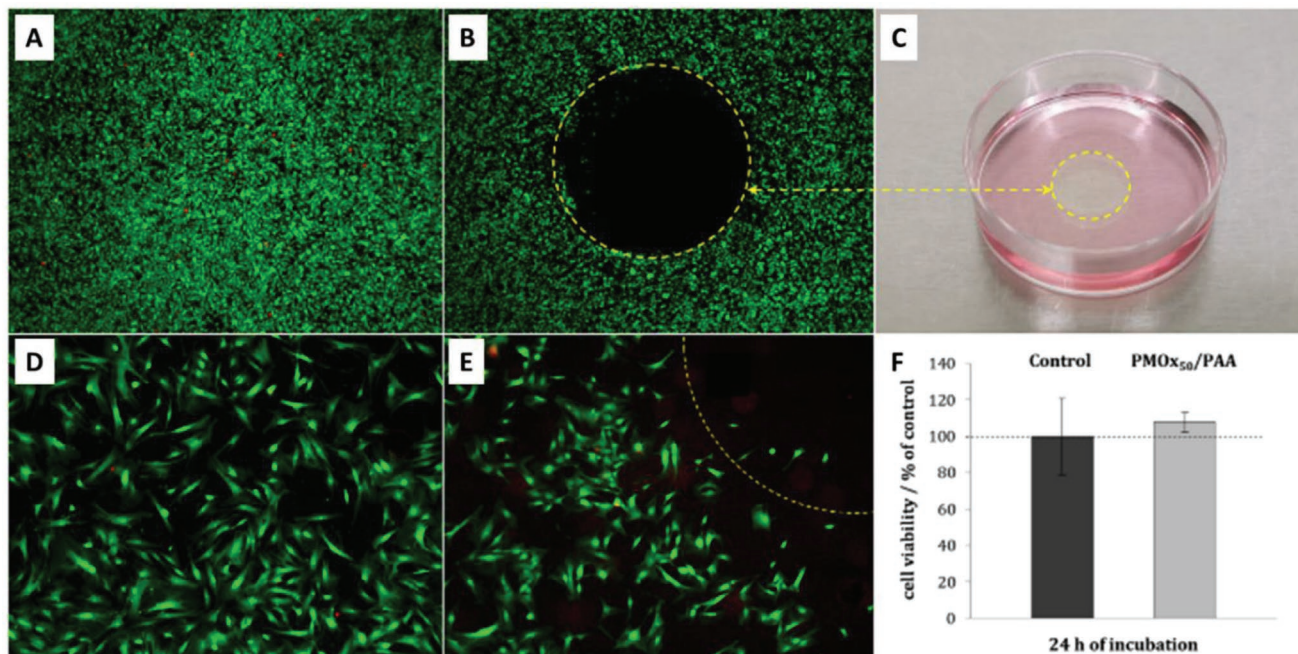


**Figure 8.** Cell morphology and viability of hMSC in the presence of PMOx<sub>50</sub>/PAA DNH after 24 h of incubation. Cells are stained with calcein-AM (green fluorescence) and PI (red fluorescence) to visualize the morphology of live and dead cells, respectively. A,D) Representative fluorescence images of hMSC control (cultivated on a cell culture Petri dish without hydrogel). B,E) Representative fluorescence images of hMSC cultivated in the presence of PMOx<sub>50</sub>/PAA DNH. C) Representative light microscopic image of PMOx<sub>50</sub>/PAA DNH placed in the middle of a cell culture Petri dish in RPMI/FCS. F) Quantification of cell viability of hMSC performed by phase analysis of the calcein-AM staining using a region of interest. Data are expressed as mean value  $\pm$  SD of  $n \geq 3$  independent experiments and given as the percentage of hMSC control.

for 24 h. Afterwards, the samples were photographed and the viability of the cells was determined with a fluorescence assay (see Figure 8).

As seen in Figure 8B,C, the stem cells did not grow on top of the hydrogel, which is a typical and desirable feature of cartilage-like materials due to their hydrogel character. However, the cells did attach and grow to the very proximity of the DNH indicating that the material does not leach toxic components. This is also shown by the spreading of the cells, which looks very much like that of the control (see Figure 8D,E). The viability of the cells was also not affected as seen in Figure 8F. Altogether, it can be stated the PMOx<sub>50</sub>/PAA is not cytotoxic and does not allow attachment and growth of human stem cells on its surface.

### 3. Conclusion

In summary, the novel PMOx/PAA networks were developed to use the  $pK_a$  shifting effect of the combination of PAA and POx to obtain a non-ionic high-performance DNH. The resulting material is shifting the  $pK_a$  of PAA by almost three orders of magnitude, which makes the material a cartilage-like hydrogel, which does not react to environmental changes salt concentration or pH changes up to 7.4. The hydrogel is taking up to 66 wt% of water and has a two to three-fold higher compression strength than other cartilage-like materials (see Table S3, in the Supporting Information). The strong drop of mechanical

integrity also makes it a smart material with a potentially very narrow pH switching range.

### 4. Experimental Section

**Materials:** Chloroform (Fischer Scientific) was distilled from activated aluminum oxide (Merck) under reduced pressure and under argon atmosphere stored. The monomers 2-methyl-2-oxazolin (MOx) and 2-ethyl-2-oxazoline (EtOx) were obtained from Acros Organics, these were distilled over CaH<sub>2</sub> (Acros Organics). *Trans*-1,4-dibromo-2-butene (DBB, Acros Organics) was recrystallized twice from *n*-heptane (Fischer Scientific). *N*-[3-(Dimethylamino)propyl]methacrylamide (DMAP-MAA, Sigma-Aldrich) was under reduced pressure distilled. All distilled chemicals were under argon atmosphere and at  $-20^\circ\text{C}$  stored. Acrylic acid (AA, 98% extra pure, Acros Organics), Irgacure 2959 (IG2959, >98%, TCI-Europe), Irgacure 651 (IG651, Ciba Specialty Chemicals), Tetraethylene glycol dimethacrylate, (TEGDMA, Sigma-Aldrich), methanol (Fischer Scientific), diethyl ether (Honeywell Riedel-de-Haën). The phosphate buffered saline, 10 $\times$  Solution (10 $\times$  PBS, Fischer Scientific) was diluted for the measurements with distilled water to a 1 $\times$  solution (1 $\times$  PBS) with a pH value of 7.4. Egg white from fresh hen eggs. The porcine native cartilage of German Edelschwein (6–8 months old) was kindly provided from Schultenhof Dortmund, Germany.

**Synthesis of Poly(2-Oxazoline) Macromonomers with DMAP-MAA End Groups:** The synthesis of telechelic PMOx and PEtOx with different degree of polymerization was performed according to previous works of Tiller et al.<sup>[46]</sup> The cationic ring opening polymerization of 2-methyl-2-oxazolin (MOx) and 2-ethyl-2-oxazoline (EtOx) with DBB as initiator was carried out in dry chloroform (20 mL) under argon atmosphere in an industrial microwave reactor. Since die polymerization time and

**Table 1.** Composition and polymerization conditions for the synthesis of PMOx and PEOx with DMAP-MAA end groups.

Polymer	$m_{\text{-DBS}}$ [g]	$V_{\text{Monomer}}^{\text{a)}}$ [mL]	Time [h]	Temperature [°C]	$V_{\text{DMAP-MAA}}^{\text{b)}}$ [mL]
PMOx <sub>25</sub>	0.5	5	1.5	105	4.2
PMOx <sub>50</sub>	0.25	5	2.5	105	2.1
PMOx <sub>100</sub>	0.125	5	4	105	1.1
PEtOx <sub>25</sub>	0.423	5	1.5	110	3.6
PEtOx <sub>50</sub>	0.21	5	2.5	110	1.8
PEtOx <sub>100</sub>	0.106	5	4	110	0.9

<sup>a)</sup>Volume of monomer (MOx or EtOx); <sup>b)</sup>Volume of DMAP-MAA to functionalization of PMOx and PEtOx

temperature depend on the degree of polymerization and monomer's type, the polymerization time and temperature for the different polymers are in **Table 1** listed. The living ends of all polymers were terminated with *N*-[3-(Dimethylamino)propyl]methacrylamide (DMAP-MAA) in a 10-fold molar excess (respect to the initiator) at 49 °C for 72 h. The resulting polymeric product was purified by precipitating the polymers three times in ice-cold diethyl ether and then dialyzed against mixture of methanol/H<sub>2</sub>O (1:1) using benzoylated cellulose membranes (1000 MWCO). The methanol was first removed under reduced pressure and the remaining aqueous solution was dried by lyophilization.

**Fabrication of the POx/PAA DNHs:** The double networks hydrogels based on POx/PAA were synthesized via the two-step polymerization method, which was first developed by Gong et al.<sup>[31]</sup> The primary hydrogel network was prepared from an aqueous solution with 34 wt% macromonomer POx with DMAP-MAA end groups and photoinitiator IG2959 (4.6 wt% respect to the macromonomer). This precursor solution was placed between two microscope slides, which were previously coated with poly(propylene)-tape and separated by 1.05 mm thick spacers for the compression-tested samples. Spacers with 0.35 mm thickness were used for tensile-tested hydrogels, so that these could be fixed between the clamps of the tensile tester. Then, it reacted in a UV curing chamber (Emmi-Classic automatic, 36 W,  $\lambda = 340$  nm) for 36 min (switching each side every 2 min). Upon the exposure to the UV light, the macromonomer underwent a free-radical induced polymerization to form a stable POx primary network (1N). Afterwards the POx network was soaked in DI water overnight, in order to remove the unreacted macromonomers and impurities.

To incorporate the PAA-based second network, the first network was carefully removed from the water and immersed in an acrylic acid (AA) solution containing the photoinitiator IG651 (0.24 wt% with respect to AA) and tetraethylene glycol dimethacrylate (TEGDMA) as crosslinking agent (0.22 wt% with respect to AA) overnight. Afterwards, the swollen hydrogel was placed between the glass plates and cured under UV source for another 20 min (switching each side every 2 min). The final POx/PAA double network (DN) hydrogel was removed from the glass plates and washed thoroughly with water for at least 48 h. All washed DN hydrogels were dried at room temperature and given in the corresponding swelling media (H<sub>2</sub>O, PBS (pH 7.4) and egg white) at least 48 h before the measurements.

**Determination of the WC:** Four dry hydrogel samples with 6 mm diameter were weighted ( $m_{\text{d},1}$ ) and immersed in DI water, PBS (pH 7.4), and egg white, respectively, until reaching equilibrium, which corresponds to a swelling time of at least 48 h. After the samples were swelled, they were dried under vacuum at 45 °C for 48 h. In order to determine the WC by neglecting other components such as salt or protein from the swelling media, the wet ( $m_{\text{g}}$ ) and dry (after swelling,  $m_{\text{d},2}$ ) weights of the DN hydrogels were compared. The WC was calculated as follows and listed in Table S2, Supporting Information:

$$\text{WC}(\text{wt}\%) = \frac{m_{\text{g}} - m_{\text{d},2}}{m_{\text{d},2}} \times 100 \quad (1)$$

**Tensile Mechanical Test:** The tensile stress–strain–curves were recorded at room temperature using an Instron 3340 tensile tester

with a cell with load of 1 kN. At least four swelled rectangular samples of different POx/PAA networks with average dimensions of 5.2 mm × 40.0 mm × 0.76 mm (width × length × thickness) were fixed between the clamps with help of sandpaper resulting in effective lengths ( $l_0$ ) between 23 and 24 mm. The experiment was performed at a crosshead speed of 5% min<sup>-1</sup> until failure of the sample. During the whole experiment, the samples were kept hydrated with the corresponding swelling media using a spray bottle. The tensile modulus was obtained from the initial slope of the stress–strain curve.

The determination of the fracture energy was determined based on previous works of Tiller et al.<sup>[61,66]</sup> Three additional samples, with the same dimensions as mentioned above, were notched in the center. The notch length corresponds to one-third of the sample's width. The tensile test of the notched samples was performed until failure as described above. This experiment allows to determine the strain at which the notch turns into a running crack. The corresponding fracture energy ( $\Gamma$ , in J m<sup>-2</sup>) of the samples was calculated as follows:

$$\Gamma = l_0 \times \int_0^{\epsilon_f} \sigma(\epsilon) d\epsilon \quad (2)$$

**Compressive Mechanical Test:** The compressive behavior of PMOx<sub>50</sub>/PAA and native cartilage were evaluated with an Instron 5967 tester with a cell load of 30 kN at room temperature. Five circular samples with diameter of 12 mm and thickness between 1.8 and 2.2 mm, which was thickness relevant to cartilage,<sup>[67,68]</sup> were tested. The sample was placed in the compression cell, covered with swelling media (H<sub>2</sub>O, PBS, or egg white), and compressed with an initial preload of 1N. All samples were compressed with a compressive strain rate of 0.5 mm min<sup>-1</sup> until failure. Compressive stress–strain–curves were recorded. Compressive modulus values were obtained from the slope at 0.2–0.3 MPa and 2–3 MPa compressive stress, respectively.

**Viscoelasticity Test:** The viscoelastic behavior of the PMOx<sub>50</sub>/PAA hydrogel and native cartilage was performed by a Discovery Dynamic mechanical analysis (DMA) 850 (TA Instruments) with a compression submersion clamp. The DMA device allows a maximal total force of 18 N, in order to perform a creep sequenced fatigue test, a static force of 8.7 N and an additional dynamic force of 8.5 N was applied.

The swelled samples of PMOx<sub>50</sub>/PAA and native cartilage with 6 mm diameter and average thickness of 1.8 mm were placed in the submersion clamp and covered with the corresponding swelling media ( $n = 5$ ). The viscoelasticity test started with a creep test applying a total constant force of 8.7 N ( $\approx 0.3$  MPa) to simulate the standing position for 30 min. In order to simulate the gait movement, a static force of 8.7 N and an additional dynamic force of 8.5 N ( $\approx$ total stress 0.6 MPa) with a frequency of 1 Hz for another 30 min were applied. A frequency of 1 Hz has been reported as characteristic gait frequency. Afterwards, the material was kept at 0.3 MPa for 3 min (stand) and then the load was removed. The thickness of the material was measured after 1 and 1800 s. In addition, stress–strain curves of the samples before and after the viscoelasticity test were recorded with a strain rate of 0.5 mm min<sup>-1</sup>. The compressions moduli were calculated from the slope of the curves at 0.2–0.3 MPa.

**Tribological Test:** The COF of the PMOX<sub>50</sub>/PAA DNH was determined by a ball on disc tribometer (CSM Instruments, Switzerland) with an Al<sub>2</sub>O<sub>3</sub> ball (*D* = 6 mm) as counter body. The PMOX<sub>50</sub>/PAA were soaked in PBS (pH 7.4) and in egg white, respectively, at least for 48 h before performing the tribological tests. Hydrogel disks with 30 mm in diameter were selected and an additional lubrication of 2 mL of the corresponding lubricant (PBS or egg white) was added. The tests were performed with a sliding speed of 5 mm s<sup>-1</sup> applying a normal load of 5 N (equivalent to a Hertzian contact pressure of 1.2 MPa) which was in the range of the joint contact stress range (0.1–5 MPa).<sup>[57]</sup> The tribological test was performed for 375 rotations using a data acquisition frequency of 10 Hz.

**Cytocompatibility:** The cytocompatibility properties of the produced PMOX<sub>50</sub>/PAA DNH were analyzed using hMSC (Lonza, Basel, Switzerland). Cultivation of hMSC was performed in RPMI/FCS (RPMI1640 (GIBCO, Invitrogen, Karlsruhe, Germany) containing 10% fetal calf serum (FCS; GIBCO) and 0.3 g L<sup>-1</sup> L-glutamine using 75 cm<sup>2</sup> culture flasks (BD Falcon, Becton Dickinson GmbH, Heidelberg, Germany) in a humidified 5% CO<sub>2</sub> atmosphere at 37 °C (standard cell culture conditions), while sub-cultivation was performed every 7 to 14 days depending on cell proliferation. For cell culture experiments, adherent sub-confluently growing hMSC were washed with phosphate-buffered saline solution (PBS; GIBCO) and detached from cell culture flasks by 5 min of incubation with 0.2 mL cm<sup>-2</sup> 0.25% trypsin/0.05% ethylenediaminetetraacetic acid (EDTA, Sigma-Aldrich, Taufkirchen, Germany) at 37 °C. Detached cells were harvested and washed twice with RPMI/FCS.

Prior to biological testing, PMOX<sub>50</sub>/PAA hydrogel disks with a diameter of 10 mm were stamped using a biopsy punch, and washed extensively in cell culture medium RPMI/FCS. Afterwards the DNHS were sterilized by 30 min of UV irradiation (UVC 500; Hoefer, Inc., Holliston, MA, USA). Sterilized hydrogel disks were placed in the middle of cell culture Petri dishes (8.8 cm<sup>2</sup> culture area; Thermo Fisher Scientific, Waltham, USA) and hMSC were seeded at a density of 5 × 10<sup>4</sup> cells per mL and a total volume of 3 mL.

After 24 h of incubation, the Live-Dead assay was performed. For qualitative analysis of cell viability and morphology living cells were stained with 1 μM calcein-acetoxymethylester (calcein-AM; Calbiochem, Schwalbach, Germany; 30 min, 37 °C) and dead cells with 50 μg per mL propidium iodide (PI; Sigma-Aldrich; 10 min, RT) and the staining was analyzed by fluorescence microscopy (Olympus MVX10, Olympus, Hamburg, Germany). Quantification of cell viability was performed by phase analysis (CellSens Dimensions, Olympus). Therefore a region of interest (ROI) was set at the location of the hydrogel within the culture dish (Figure S9A, Supporting Information) and the remaining calcein-fluorescent area was obtained by subtracting the area of the ROI (Figure S9C minus S9B and S9F minus S9E, Supporting Information). The data were given as percentage of a cell control area (hMSC cultivated in cell culture Petri dishes without hydrogel), which was set as 100%.

**Statistical Analysis:** All values were expressed as mean ± standard deviation (SD). The results were analyzed statistically using a one-way ANOVA, followed by a Tukey post-hoc test. In all cases, the significance was set at *p* ≤ 0.05. Statistical analysis was carried out using OriginPro 2020b Software.

## Supporting Information

Supporting Information is available from the Wiley Online Library or from the author.

## Acknowledgements

The authors thank Dr. Wolf Hiller and his team (department of chemistry, TU Dortmund) for recording the NMR spectra. The authors also thank Dr. Frank Katzenberg und Thorsten Moll for their assistance with mechanical testing. All polymers were synthesized using CEM

Discover microwaves, which were kindly provided by CEM GmbH for undergraduate student education. The authors also thank the organic farm Schultenhof, Dortmund, for providing the porcine cartilage and Ciba Specialty Chemicals (part of BASF) for providing Irgacure 651.

Open access funding enabled and organized by Projekt DEAL.

## Conflict of Interest

The authors declare no conflict of interest.

## Author Contributions

J.C.T. and P.A.B.-D. designed the study, interpreted the results, and wrote the manuscript. P.A.B.-D., D.K., S.G., and K.E. prepared the hydrogels, performed the mechanical tests and swelling experiments. M.B. conducted the biocompatibility test. W.T. and D.S. assisted with the tribological test, which was performed by P.A.B.-D., D.K., and M.H. assisted with the preliminary design and fabrication of hydrogels, and the enzyme degradation test.

## Data Availability Statement

The data that support the findings of this study are available in the supplementary material of this article.

## Keywords

cartilage, double-network hydrogels, poly(2-oxazoline), poly(acrylic acid)

Received: April 28, 2022

Revised: July 12, 2022

Published online: August 11, 2022

- [1] D. J. Hunter, S. Bierma-Zeinstra, *Lancet* **2019**, 393, 1745.
- [2] D. J. Hunter, L. March, M. Chew, *Lancet* **2020**, 396, 1711.
- [3] W. Wei, Y. Ma, X. Yao, W. Zhou, X. Wang, C. Li, J. Lin, Q. He, S. Leptihn, H. Ouyang, *Bioact. Mater.* **2021**, 6, 998.
- [4] C. M. Beddoes, M. R. Whitehouse, W. H. Briscoe, B. Su, *Materials* **2016**, 9, 443.
- [5] Y. Krishnan, A. J. Grodzinsky, *Matrix Biol.* **2018**, 71–72, 51.
- [6] F. Yang, J. Zhao, W. J. Koshut, J. Watt, J. C. Riboh, K. Gall, B. J. Wiley, *Adv. Funct. Mater.* **2020**, 30, 2003451.
- [7] A. J. Kerin, M. R. Wisnom, M. A. Adams, *Proc. Inst. Mech. Eng., Part H* **1998**, 212, 273.
- [8] D. Warnecke, M. Meßmer, L. de Roy, S. Stein, C. Gentilini, R. Walker, N. Skaer, A. Ignatius, L. Dürselen, *Sci. Rep.* **2019**, 9, 5785.
- [9] H. Forster, J. Fisher, *Proc. Inst. Mech. Eng., Part H* **1999**, 213, 329.
- [10] A. K. Means, M. A. Grunlan, *ACS Macro Lett.* **2019**, 8, 705.
- [11] L. Trachsel, C. Johnbosco, T. Lang, E. M. Benetti, M. Zenobi-Wong, *Biomacromolecules* **2019**, 20, 4502.
- [12] A. K. Means, C. S. Shrode, L. V. Whitney, D. A. Ehrhardt, M. A. Grunlan, *Biomacromolecules* **2019**, 20, 2034.
- [13] Q. Chen, H. Chen, L. Zhu, J. Zheng, *J. Mater. Chem. B* **2015**, 3, 3654.
- [14] A. Strassburg, J. Petranowitsch, F. Paetzold, C. Krumm, E. Peter, M. Meuris, M. Köller, J. C. Tiller, *ACS Appl. Mater. Interfaces* **2017**, 9, 36573.
- [15] N. Rauner, M. Meuris, M. Zoric, J. C. Tiller, *Nature* **2017**, 543, 407.
- [16] M. Milovanovic, L. Mihailowitsch, M. Santhirasegaran, V. Brandt, J. C. Tiller, *J. Mater. Sci.* **2021**, 56, 15299.

- [17] Y. Meng, L. Ye, P. Coates, P. Twigg, *J. Phys. Chem. C* **2018**, 122, 3157.
- [18] E. C. Beck, M. Barragan, M. H. Tadros, S. H. Gehrke, M. S. Detamore, *Acta Biomater.* **2016**, 38, 94.
- [19] J. P. Gong, *Soft Matter* **2010**, 6, 2583.
- [20] C. Azuma, K. Yasuda, Y. Tanabe, H. Taniguro, F. Kanaya, A. Nakayama, Y. M. Chen, J. P. Gong, Y. Osada, *J. Biomed. Mater. Res., Part A* **2007**, 81A, 373.
- [21] K. Yasuda, J. P. Gong, Y. Katsuyama, A. Nakayama, Y. Tanabe, E. Kondo, M. Ueno, Y. Osada, *Biomaterials* **2005**, 26, 4468.
- [22] M. P. Arnold, A. U. Daniels, S. Ronken, H. A. García, N. F. Friederich, T. Kurokawa, J. P. Gong, D. Wirz, *Cartilage* **2011**, 2, 374.
- [23] S. Ronken, D. Wirz, A. U. Daniels, T. Kurokawa, J. P. Gong, M. P. Arnold, *Biomech. Model. Mechanobiol* **2013**, 12, 243.
- [24] N. Ding, X. Cai, P. Zhang, S. Dong, B. Du, J. Nie, P. Yu, *ACS Appl. Polym. Mater.* **2021**, 3, 2709.
- [25] Y. Cheng, Y. Hu, M. Xu, M. Qin, W. Lan, D. Huang, Y. Wei, W. Chen, *J. Biomater. Sci., Polym. Ed.* **2020**, 31, 1836.
- [26] D. A. Bichara, H. Bodugoz-Sentruk, D. Ling, E. Malchou, C. R. Bragdon, O. K. Muratoglu, *Biomed. Mater.* **2014**, 9, 045012.
- [27] S. Pourbashir, M. Shahrourvand, M. Ghaffari, *Int. J. Biol. Macromol.* **2020**, 142, 298.
- [28] D. Myung, W. Koh, J. Ko, Y. Hu, M. Carrasco, J. Noolandi, C. N. Ta, C. W. Frank, *Polymer* **2007**, 48, 5376.
- [29] X. W. Xu, V. V. Jerca, R. Hoogenboom, *Mater. Horiz.* **2021**, 8, 1173.
- [30] X. Zhao, J. Liang, G. Shan, P. Pan, *J. Mater. Chem. B* **2019**, 7, 324.
- [31] J. P. Gong, Y. Katsuyama, T. Kurokawa, Y. Osada, *Adv. Mater.* **2003**, 15, 1155.
- [32] D. Myung, D. Waters, M. Wiseman, P.-E. Duhamel, J. Noolandi, C. N. Ta, C. W. Frank, *Polym. Adv. Technol.* **2008**, 19, 647.
- [33] J. You, S. Xie, J. Cao, H. Ge, M. Xu, L. Zhang, J. Zhou, *Macromolecules* **2016**, 49, 1049.
- [34] L. Hartmann, K. Watanabe, L. L. Zheng, C. Y. Kim, S. E. Beck, P. Huie, J. Noolandi, J. R. Cochran, C. N. Ta, C. W. Frank, *J. Biomed. Mater. Res., Part B* **2011**, 98, 8.
- [35] T. Liu, C. Jiao, X. Peng, Y.-N. Chen, Y. Chen, C. He, R. Liu, H. Wang, *J. Mater. Chem. B* **2018**, 6, 8105.
- [36] L. L. Zheng, V. Vanchinathan, R. Dalal, J. Noolandi, D. J. Waters, L. Hartmann, J. R. Cochran, C. W. Frank, C. Q. Yu, C. N. Ta, *J. Biomed. Mater. Res., Part A* **2015**, 103, 3157.
- [37] S. Naficy, J. M. Razal, P. G. Whitten, G. G. Wallace, G. M. Spinks, *J. Polym. Sci., Part B: Polym. Phys.* **2012**, 50, 423.
- [38] T. He, D. Jarczywski, S. Guo, S. M. Man, S. Jiang, W. S. Tan, *Colloids Surf., B* **2018**, 161, 269.
- [39] V. Kozlovskaya, A. Shamaev, S. A. Sukhishvili, *Soft Matter* **2008**, 4, 1499.
- [40] Y. Li, T. Pan, B. Ma, J. Liu, J. Sun, *ACS Appl. Mater. Interfaces* **2017**, 9, 14429.
- [41] C. Su, J. Sun, X. Zhang, D. Shen, S. Yang, *Polymers* **2017**, 9, 363.
- [42] N. Mathivanan, G. Paramasivam, M. Vergaalen, J. Rajendran, R. Hoogenboom, A. Sundaramurthy, *Langmuir* **2019**, 35, 14712.
- [43] C. Krumm, S. Konieczny, G. J. Dropalla, M. Milbradt, J. C. Tiller, *Macromolecules* **2013**, 46, 3234.
- [44] I. Schoenfeld, S. Dech, B. Ryabenky, B. Daniel, B. Glowacki, R. Ladisch, J. C. Tiller, *Biotechnol. Bioeng.* **2013**, 110, 2333.
- [45] I. Sittko, K. Kremser, M. Roth, S. Kuehne, S. Stuhr, J. C. Tiller, *Polymer* **2015**, 64, 122.
- [46] S. A. Wilhelm, M. Maricanov, V. Brandt, F. Katzenberg, J. C. Tiller, *Polymer* **2022**, 242, 124582.
- [47] R. Knauss, J. Schiller, G. Fleischer, J. Kärger, K. Arnold, *Magn. Reson. Med.* **1999**, 41, 285.
- [48] C. Liess, S. Lüsse, N. Karger, M. Heller, C. C. Glüer, *Osteoarthritis and Cartilage* **2002**, 10, 907.
- [49] S. Akizuki, V. C. Mow, F. Müller, J. C. Pita, D. S. Howell, D. H. Manicourt, *J. Orthop. Res.* **1986**, 4, 379.
- [50] R. M. Natoli, C. M. Revell, K. A. Athanasiou, *Tissue Eng., Part A* **2009**, 15, 3119.
- [51] S. G. Cook, Y. Guan, N. J. Pacifici, C. N. Brown, E. Czako, M. S. Samak, L. J. Bonassar, D. Gourdon, *Langmuir* **2019**, 35, 15887.
- [52] A. Faryna, K. Goldenberg, in *Clinical Methods: The History, Physical, and Laboratory Examinations*, (Eds.: H. K. Walker, W. D. Hall, J. W. Hurst), Butterworth Publishers, Boston **1990**, p. 774.
- [53] S. Jahn, J. Seror, J. Klein, *Annu. Rev. Biomed. Eng.* **2016**, 18, 235.
- [54] L. Fu, X. Sun, W. He, C. Cai, A. Onishi, F. Zhang, R. J. Linhardt, Z. Liu, *Glycobiology* **2016**, 26, 693.
- [55] M. Hayashi, K. Kadomatsu, T. Kojima, N. Ishiguro, *Biochem. Biophys. Res. Commun.* **2011**, 409, 732.
- [56] Z. Liu, F. Zhang, L. Li, G. Li, W. He, R. J. Linhardt, *Glycoconjugate J.* **2014**, 31, 593.
- [57] R. A. Brand, *Iowa Orthop J* **2005**, 25, 82.
- [58] F. Guilak, *Arthritis Rheum.* **2005**, 52, 1632.
- [59] B. M. Lawless, H. Sadeghi, D. K. Temple, H. Dhaliwal, D. M. Espino, D. W. L. Hukins, *J. Mech. Behav. Biomed. Mater.* **2017**, 75, 293.
- [60] B. Grabowska, M. Holtzer, *Arch. Metall. Mater.* **2009**, 427.
- [61] M. Milovanovic, N. Isselbacher, V. Brandt, J. C. Tiller, *Chem. Mater.* **2021**, 33, 8312.
- [62] C. P. Fik, S. Konieczny, D. H. Pashley, C. J. Waschinski, R. S. Ladisch, U. Salz, T. Bock, J. C. Tiller, *Macromol. Biosci.* **2014**, 14, 1569.
- [63] M. Hijazi, C. Krumm, S. Cinar, L. Arns, W. Alachraf, W. Hiller, W. Schrader, R. Winter, J. C. Tiller, *Chem. - Eur. J.* **2018**, 24, 4523.
- [64] S. Konieczny, C. P. Fik, N. J. H. Aversch, J. C. Tiller, *J. Biotechnol.* **2012**, 159, 195.
- [65] S. Konieczny, C. Krumm, D. Doert, K. Neufeld, J. C. Tiller, *J. Biotechnol.* **2014**, 181, 55.
- [66] M. Milovanovic, N. Rauner, E. Civelek, T. Holtermann, O. E. Jid, M. Meuris, V. Brandt, J. C. Tiller, *Macromol. Mater. Eng.* **2022**, <https://doi.org/10.1002/mame.202200051>.
- [67] D. E. Shepherd, B. B. Seedhom, *Ann. Rheum. Dis.* **1999**, 58, 27.
- [68] R. F. Shah, A. M. Martinez, V. Pedoia, S. Majumdar, T. P. Vail, S. A. Bini, *J. Arthroplasty* **2019**, 34, 2210.